stellarator news

Published by Fusion Energy Division, Oak Ridge National Laboratory
Building 9201-2 P.O. Box 2009 Oak Ridge, TN 37831-8071, USA

Editor: James A. Rome Issue 56 March 1998
E-Mail: jar@ornl.gov Phone (423) 574-1306 Fax: (423) 241-6211
On the Web at *http://www.ornl.gov/fed/stelnews*

First experiments on ion Bernstein wave heating in the L-2M stellarator

The ion Bernstein wave (IBW) is excited through conversion from the electron plasma wave at the periphery of the plasma column, when the generator frequency is equal to the lower hybrid frequency. Further, the IBW propagates toward the center of the plasma column and is absorbed in either the ion cyclotron resonance region or the resonance regions for harmonics of the ion cyclotron frequency.

The aim of this work is the experimental study and comparative analysis of characteristic features of IBW heating in stellarators; it was carried out in the L2-M stellarator, which is located at the General Physics Institute of the Russian Academy of Sciences.

To excite IBWs we used a longitudinal antenna, the so-called Nagoya Type III (Fig. 1), covered by a double electrostatic shield. A current-carrying loop of this antenna was oriented along the outer wall of the toroidal chamber in the equatorial plane. The antenna was shaped so that the distance from the shield to the plasma was everywhere

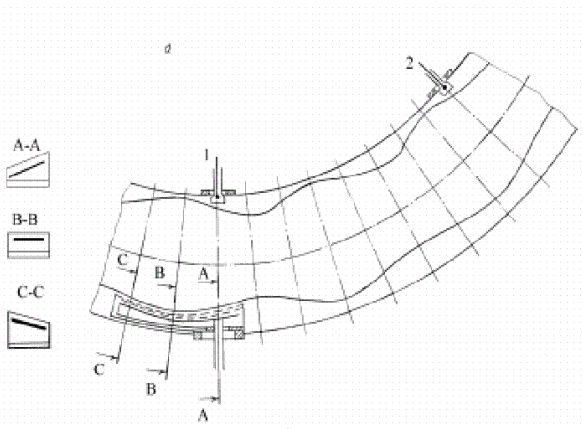

Fig. 1. Experimental layout. Shown are three sections through the antenna and the locations of two magnetic probes (1, 2).

In this issue . . .

equal to 1 cm (Fig. 1). Near the antenna, magnetic field lines are inclined to its longitudinal axis by small angles, and the inclination varies along the antenna. The maximum poloidal angle between the magnetic field line and the direction of the antenna current is 15°. The generator frequency was 20 MHz, and the pulse duration was 3 ms.

The presence of the current component perpendicular to the magnetic field line can lead to the excitation of fast magnetosonic waves (FMSWs). Measurements of the magnetic field component B_z by magnetic probes (the distance between the probes in Fig. 1 is 0.9 m) showed that, under our conditions, the toroidal antenna excited FMSW of small amplitude, i.e., about 5–10 times smaller than that observed in previous experiments with a poloidal antenna under similar conditions [1].

The energy spectrum of the hydrogen ions was measured by a 5-channel charge-exchange particle analyzer.

In the Ohmic discharge [I_{OH} = 13–18 kA, with an average density $n_e = 1 \times 10^{19}$ m^{-3}, $T_e(0)$ = 200–350 eV, and $T_i(0)$ = 50–80 eV], ion heating was observed only at the frequencies $\omega = \omega_{ci}$ (B = 1.32 T) and $\omega = 3/2\omega_{ci}$ (B = 0.88 T), whereas no heating was observed at $\omega_{ci} < \omega < 3/2\omega_{ci}$. In both cases where additional ion heating was observed, the central ion temperature increased by $\Delta T_i(0)$ = 40 eV, and the time behavior $\Delta T_i(t)$ was identical. The absorbed RF power was P = 20 kW, limited by coupling of the antenna to plasma.

In the "currentless" electron cyclotron (ECR) heated plasma [$T_e(0)$ = 0.8 keV; $T_i(0)$ = 100 eV; $n_e = 0.7 \times 10^{19}$ m^{-3}], the additional ion heating was observed at $\omega = \omega_{ci}$. In this case, however, the heating power decreased from 20 to 14 kW during the heating pulse. The maximum growth in the ion temperature was observed at the beginning of the heating pulse, and the central temperature increased by $\Delta T_i(0)$ = 40 eV.

In all cases where additional ion heating was observed, the ion energy spectra corresponded to Maxwellian energy distributions.

The experiments showed that the efficiency of the IBW heating was actually the same at both frequencies, $\omega = \omega_{ci}$ and $\omega = 3/2\omega_{ci}$. Comparison of the two regimes of IBW heating (i.e., of the ohmically and ECR created plasmas) showed that, although the maximum value of ΔT_i was the same in both regimes, the time history of heating was different. Before the RF power was switched on, the plasma parameters differed substantially in these two regimes. Thus, the electron temperature of the ECR-heated plasma was higher than that of the ohmically heated plasma by a factor of 3 in the center, and it was higher by a factor of 2 near the separatrix. The RF power was constant during the IBW heating pulse in the ohmic discharge and decreased in the ECR-heated plasma, which indicates less effective coupling in the latter case.

As mentioned above, we observed small-amplitude FMSWs in these experiments. Our previous experiments indicate the high efficiency of FMSW heating in hydrogen plasmas at the fundamental harmonic of the ion cyclotron frequency [1]. For this reason, the evaluation of the individual contributions from the IBW and FMSW to ion heating presents difficulty.

In comparing the IBW heating efficiencies at the frequencies $\omega = \omega_{ci}$ and $\omega = 3/2\omega_{ci}$, one should take into account that the experiments were carried out at different magnetic fields, 1.3 and 0.8 T, respectively. The lower the magnetic field, the shorter the ion energy confinement time. It is obvious that, for a correct comparison of IBW heating at these two frequencies, it is desirable to carry out the experiments at the same magnetic field by varying the generator frequency. Unfortunately, it was impossible for technical reasons in these experiments.

The observed ion heating at the frequency $\omega = 3/2\omega_{ci}$ is evidence that IBWs are excited in the plasma. The ion heating efficiency is η = 1.5 eV/kW for am average plasma density $n_e = 1 \times 10^{19}$ m^{-3}.

References:

[1] V.A. Batyuk, G.S. Voronov, E.F Gippius. et al., Sov. J. Plasma Phys. **13** (1987) 143.

A. Meshcheryakov and the L-2M Team
General Physics Institute, Russian Academy of Sciences
Moscow, Russia

E-mail: meshch@fpl.gpi.ru
FAX: 095-1358011

Electric field bifurcation and transition in the core plasma of CHS

In the Compact Helical System (CHS) heliotron/torsatron, the statics and dynamics of potential are investigated with a heavy-ion beam probe (HIBP). In toroidal helical systems, transport can be enhanced by helically trapped particles, which are intrinsically affected by the radial electric field. Here, we describe observations of a spontaneous transition in the radial electric field in CHS and present the nonlinear relationship between radial electric field and current which is responsible for the bifurcation.

Eexperiments were performed in a 0.9-T magnetic field configuration whose axis is located at R_{ax} = 92.1 cm. In this configuration the HIBP uses a cesium beam at an injection energy of 71 keV, resulting in a radial resolution of about a few centimeters. The observation location of HIBP can be altered by sweeping the voltages controlling the beam trajectory. The time evolution of the potential profile can be observed either in this radial scan mode or with a temporal resolution of 450 kHz if a single position is probed (fixed-sweep mode).

Transition phenomena in the radial electric field have been observed in low-density CHS plasmas with combined electron cyclotron heating (ECH) and neutral beam injection (NBI). For example, in a deuterium plasma with 300 kW of ECH (300 kW) and port-through NBI power of 800 kW. During the combined heating phase the line-averaged electron density rises from $n_e = 3 \times 10^{12}$ cm^{-3} to $n_e = 6 \times 10^{12}$ cm^{-3}. The central electron temperatures are 800 ± 200 eV as measured by Thomson scattering. The ion temperatures are expected to increase from 100 eV to 300 eV. Figure 1 shows the evolution of the potential during the combined phase of the discharge. Data are taken in the fixed-sweep mode of the HIBP using a sequence of identical discharges. At t = 55 ms the potential at the plasma

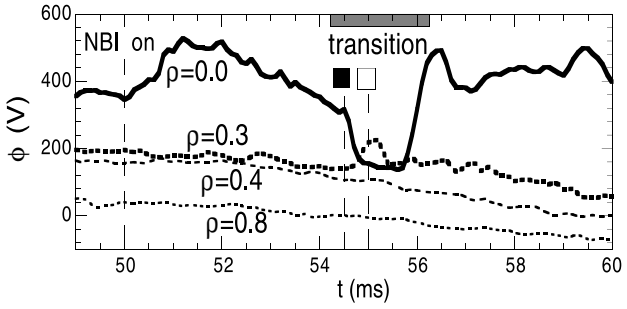

Fig. 1. Time evolution of potentials at several radii in the combined ECH+NBI heating phase. A transition in the potential at the plasma center occurs around t = 55 ms.

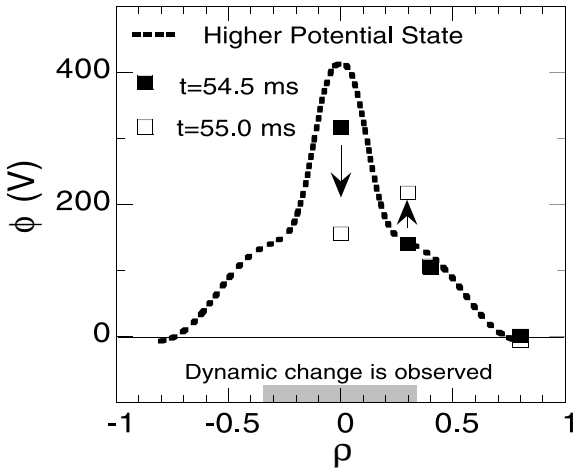

Fig. 2. Structural change in potential profile during the transition. The closed and open squares indicate the potential changes observed in measurements at the two times indicated in Fig. 1.

center $\varphi(0)$ exhibits a drastic drop of 200 V followed by an abrupt rise about 1 ms later. Fitting a function of $\tanh[(t - t_0)/\tau]$ to the slopes, one obtains time scales of τ = 60 μs for the drop and τ = 220 μs for the rise. This time scale is much faster than the confinement time, which is a few milliseconds. At normalized radius $\rho \approx 0.3$, another rise and drop are observed. The closed and open squares in Fig. 2 represent potential values just before (t = 54.5 ms) and after (t = 55.0 ms) the transition, respectively. The measurements indicate that the structural change of the transition is localized in the plasma core, $\rho < 0.4$. The profile indicated by the bold dashed line is obtained by fitting to data taken from the same sequence of discharges. This profile of the higher potential state exhibits a unique feature: the electric field (e.g., its derivative) changes drastically inside and outside ρ = 0.4. This steep gradient change suggests a momentum transport barrier. Profiles with this feature have been also been observed in plasmas with only ECH heating of 200 to 300 kW.

These temporal and spatial measurements of the electric potential allow us to evaluate the nonlinear relation of the radial current and the radial electric field E_r. The latter is obtained as $\bar{E}_r = -[\varphi(0.3a) - \varphi(0)]/0.3a$ from the measured potential assuming that $\varphi(0.3a) = \text{const.}$ The radial current is derived from Poisson's equation under the assumption of charge conservation as $\varepsilon_\perp \varepsilon_0 (\partial E_r/\partial t) = -j_r$, where $\varepsilon_\perp$ and ε_0 represent the perpendicular and vacuum dielectric constants, respectively. In this case, $\varepsilon_\perp \cong 2.7 \times 10^4$ around the plasma core. In Fig. 3(a) the relation between E_r and j_r is plotted as obtained by using the time evolution of the central potential $\varphi(0)$ in Fig. 1.

A rough comparison of these observations with neoclassical theory should be of some interest. The relationship between the radial current and the electric field to show

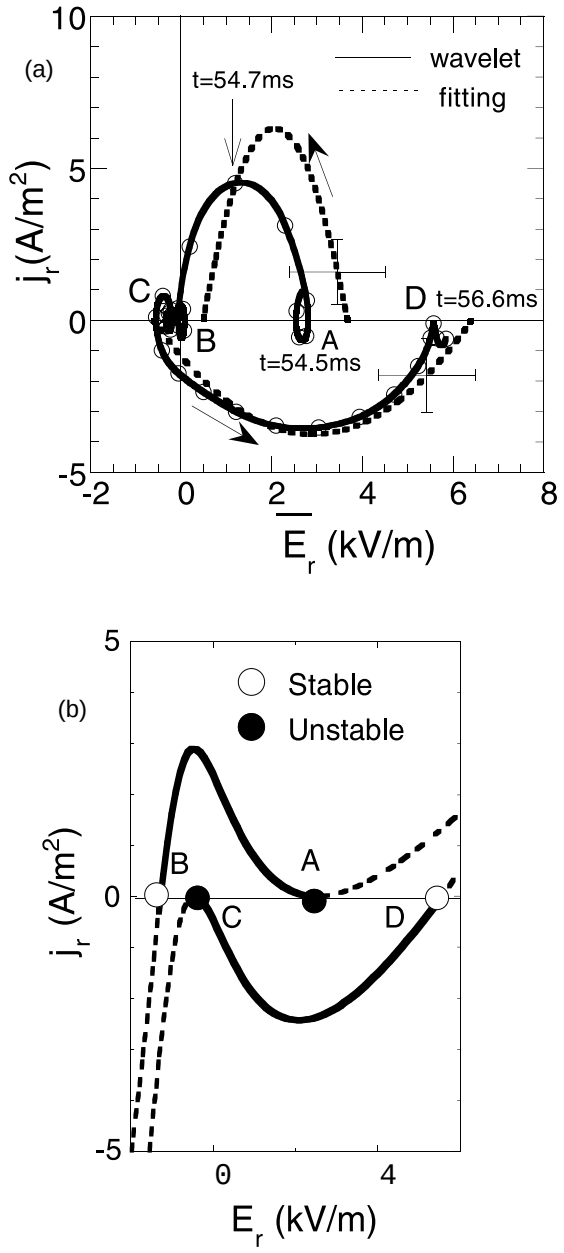

Fig. 3. Relationship between the radial electric field and the radial current.
(a) Experimental observations. The two curves for each transition are obtained by different methods to evaluate the electric field: wavelet analysis (solid line) and fitting method using $\tanh[(t - t_0)/\tau]$ (dashed line). The arrows represent the direction of transition. The circles are plotted every 64 μs.The error bars in the electric field and the radial current result from the uncertainty of the potential change at ρ = 0.3.
(b) Calculations for the corresponding bifurcation conditions. The plasma parameters used in the calculation are T_i = 350 eV, $n_e = 5 \times 10^{12}$ cm^{-3}, $(\partial T/\partial\rho)/T = -0.6$, and $(\partial n/\partial\rho)/n = -0.3$.

bifurcation characteristics can be found within the probable parameters of the CHS plasma. Examples are plotted in Fig. 3(b). Plasma parameters used in the calculation are plausible for the experimental conditionS: T_i = 350 eV, $n_e = 5 \times 10^{12}$ cm^{-3}, $(\partial T/\partial\rho)/T = -0.6$, and $(\partial n/\partial\rho)/n = -0.3$. The other parameters, such as ε_h and ε_t, are selected for ρ = 0.3 in CHS. Multiple steady states are allowed when the electron temperature ranges from 630 eV to 725 eV; the electron temperature is experimentally inferred to have a sharply peaked profile with a central value of approximately 800 eV. The maximum current to induce the transition is a few A/m^2, which is also within the experimental observations. Further investigations and accurate measurements of basic plasma parameters are essential for conclusive comparison.

In conclusion, we have observed for the first time a transition in the radial electric field in a plasma with rapid temporal evolution. The observation will contribute to understanding of the formation of improved confinement modes indicating bifurcation characteristics.

A. Fujisawa
National Institute for Fusion Science
Oroshi-cho, Toki-shi, 509-52 Japan

Completion of construction of the main LHD device

The Large Helical Device (LHD) construction team is very happy to announce that at the end of January, the construction of the main LHD device was completed almost on time. The main LHD systems (e.g., vacuum and cooling) are undergoing a series of tests. Figure 1 shows the moment when the leak test of the plasma vacuum vessel was completed. The electron cyclotron resonance (ECR) antennas were installed from the upper ports in order to produce the first plasma, and the transmission of microwave power was tested using a dummy load. The neutral beam injectors are in their final stage of construction. Experiment utilities, such as the high-pressure air system for the operation of valves, are all almost completed.

The LHD vacuum pumping system consists of two parts: one to pump the plasma vacuum vessel for producing plasmas, and one for the cryostat to provide vacuum thermal isolation. The manifolds with diameters of 1200 mm, shown in Fig. 1, and 800 mm are connected to the plasma vacuum vessel and cryostat, respectively. Pumps are connected to these manifolds: the former has two cryogenic pumps with water pumping speeds of 70,000 L/s, two turbomolecular pumps with pumping speeds of 5,000 L/s, and two compound turbomolecular pumps with pumping speeds of 1,800 L/s, while the latter has two cryogenic pumps with water pumping speeds of 25,000 L/s and two compound turbomolecular pumps with pumping speeds of 5,500 L/s.

Because of the large volume (the plasma vacuum vessel is 210 m^3 and the cryostat is 580 m^3), two oil rotary pumps with pumping speeds of 900 m^3/h are used in common for first roughing, and then two mechanical booster pumps with pumping speeds of 1630 m^3/h are used independently. Two mass spectrometers are available to monitor water and helium gas. Almost all valves and all pumps are controlled remotely by intelligent sequencers and operated from the LHD control building.

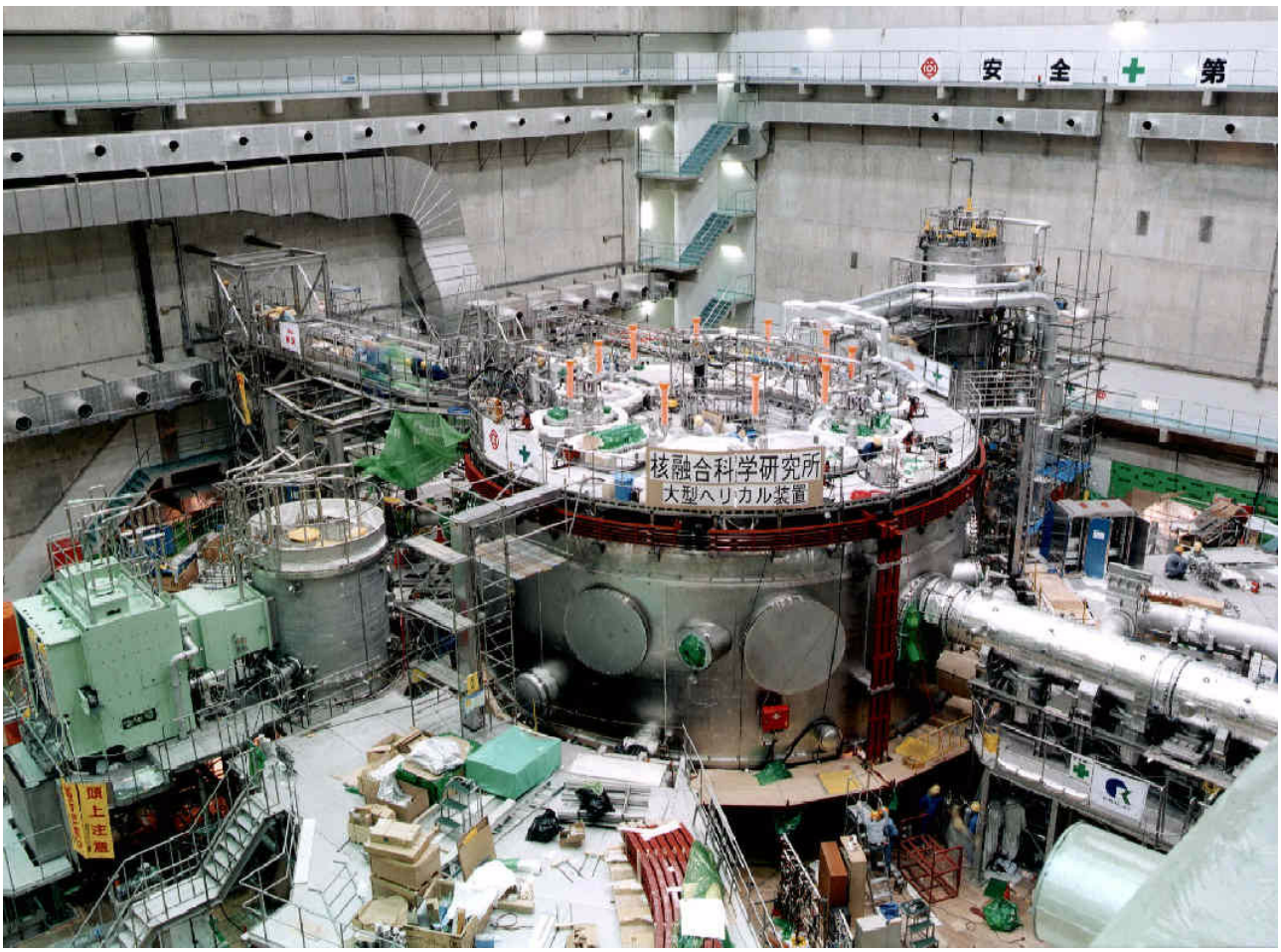

Fig. 1. The LHD at the completion of leak tesing of the plasma vacuum vesse.

Vacuum tests of the cryostat began on Tuesday, 20 January, although the plasma vacuum vessel was left open for the work of setting thermocouples on it. Figure 2 shows the time dependence of the cryostat pressure. During these tests on 20 January, the cryostat pressure decreased rapidly as time passed. However, the slope of the pressure vs time became gentle at about 1000 Pa because of outgassing and was almost flat at about 200 Pa. At this point we filled the cryostat with dry nitrogen gas and then left it alone for 12 hours. We pumped the nitrogen gas out of the cryostat the next day, and the cryostat pressure reached about 20 Pa when the slope of the pressure vs time became almost flat, as shown in Fig. 2. This pressure was lower than that obtained the day before by one order of magnitude. In this way we could achieve a cryostat pressure of about 0.02 Pa within 4 days, which is low enough for the cooldown of LHD. The main species of the desorbed gas was found to be water, as expected. Helium leak detection revealed a few small leaks in the helium cooling pipes that are located inside the cryostat and used for the cooldown. These were stopped up, and no leak remains in the cryostat in the range 10^{-8} Pa·m^3/s.

The construction of the plasma vacuum vessel was completed on Wednesday, 28 January, and the vacuum tests of the cryostat began on Friday, 30. Figure 3 shows the inside of the completed plasma vacuum vessel. There are two grooves, each 1-m wide, for one pair of helical coils; hence, the plasma vacuum vessel is helically twisted and rather complex, as shown in Fig. 3. The person in the vessel is about 1.67 m tall, and one of the outer horizontal ports can be seen near him. Water cooling pipes can be also seen, located on the plasma vacuum vessel surface that faces the plasma. Heat flux from the core plasma reaches the divertor plates and the first wall of the plasma vacuum vessel, so they must be cooled by a water cooling system. The first wall will be installed in the near future. Successful heat removal from the plasma vacuum vessel and the divertor plates is one of the important conditions for stable operation of a superconducting coil system and production of high-quality plasmas. The pressure of the plasma vacuum vessel reached 3×10^{-5} Pa within a day from the pressure of the atmosphere, and no leak was found in the plasma vacuum vessel itself and water cooling pipes in the range 10^{-9} Pa·m^3/s. At the end of February the pressure in the plasma vacuum vessel was about 7×10^{-6} Pa. Baking of the plasma vacuum vessel at up to 100 °C has not been performed yet, but will be done before the conditioning of the plasma vacuum vessel.

The purification of helium gas in the helium cooling pipes for the cooldown of LHD started on Saturday, 14 February. The main parts of LHD, to be cooled to 4.4–4.5 K are the helical coils, poloidal coils, and supporting structure, surrounded by the outer and inner 80 K radiation shields. The cooling test of LHD started on Monday, 23 February.

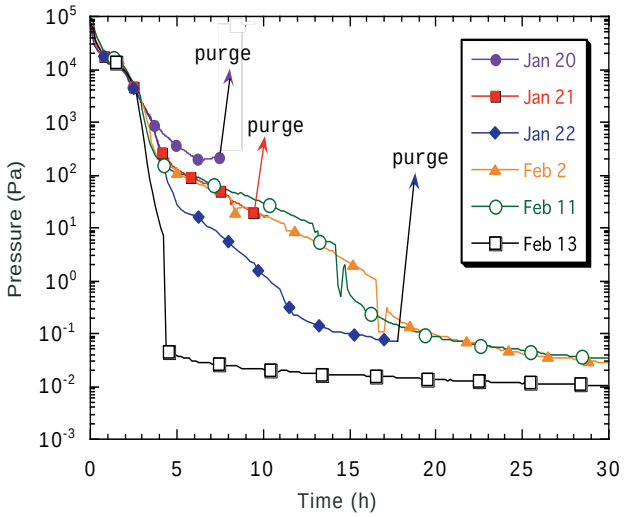

Fig. 2. Cryostat pressures as a function of time.

Fig. 3. The inside of the plasma vacuum vessel of the LHD.

LHD has been cooled by using temperature-controlled helium gas, mixing cold and warm gases in the helium refrigerator. Cooldown is in progresses at a cooling rate of about 0.8 K/h, and the inlet and outlet temperatures of the helium gas are about 150 K and 190 K, respectively. The temperature difference between the coil inlet and the coil average will be maintained at less than 50 K until the coil temperature becomes lower than 80 K. It will take about another three weeks for the coils to become cold enough for superconductivity to be realized.

Eexcitation tests of the helical and poloidal coils will be performed at the end of March immediately after the completion of the cooling test. A few days will be spent on the conditioning of the plasma vacuum vessel, using a 30-kW microwave system at 2.45 GHz. The first plasma is expected this spring.

A. Komori and the LHD Construction Team
National Institute for Fusion Science
Toki 509-5292, Japan
Phone: +81-572-58-2165
FAX: +81-572-58-2618
E-mail: komori@LHD.nifs.ac.jp